UNIVERSITÄT AUGSBURG
Universitätsbibliothek

OPEN ACCESS
OPUS AUGSBURG

Defects on proton exchange membrane fuel cell components created by particulate contaminations and mechanical pressure

Timo Schießl, Katrin Dinter, Christoph Tammer, Rüdiger Daub

Angaben zur Veröffentlichung / Publication details:

Schießl, Timo, Katrin Dinter, Christoph Tammer, and Rüdiger Daub. 2026. "Defects on proton exchange membrane fuel cell components created by particulate contaminations and mechanical pressure." *Procedia CIRP* 138: 1121–26. https://doi.org/10.1016/j.procir.2026.01.193.

Nutzungsbedingungen / Terms of use:

CC BY-NC-ND 4.0

Dieses Dokument wird unter folgenden Bedingungen zur Verfügung gestellt: / This document is made available under these conditions:
CC-BY-NC-ND 4.0: Creative Commons: Namensnennung - Nicht kommerziell - Keine Bearbeitung
Weitere Informationen finden Sie unter: / For more information see:
https://creativecommons.org/licenses/by-nc-nd/4.0/deed.de

Available online at www.sciencedirect.com

ScienceDirect

Procedia CIRP 138 (2026) 1121–1126

www.elsevier.com/locate/procedia

18th CIRP Conference on Intelligent Computation in Manufacturing Engineering

Defects on Proton Exchange Membrane Fuel Cell Components created by Particulate Contaminations and Mechanical Pressure

Timo Schießl[a]*, Katrin Dinter[a,b], Christoph Tammer[a], Rüdiger Daub[a,c]

[a]*Fraunhofer Institute for Casting, Composite and Processing Technology IGCV, Am Technologiezentrum 10, 86159 Augsburg, Germany*
[b]*Augsburg University, Faculty of Mathematics, Natural Sciences, and Materials Engineering , Universitätsstraße 2, 86159 Augsburg, Germany*
[c]*Technical Univeristy of Munich, Institute for Machine Tools and Industrial Management, Boltzmannstr. 15, 85748 Garching, Germany*

* Corresponding author. Tel.: +49-821-90678-170; fax: +49-821-90678-199. *E-mail address:* timo.schiessl@igcv.fraunhofer.de

Abstract

The technical cleanliness is a crucial quality aspect in modern production of sensible components due to the harmful properties of contaminations on these parts. The presence of particles poses a risk of damage, hence demanding high cleanliness standards for certain parts. Given the complexity of cleanliness measures, it is crucial to precisely understand the influence of contaminants to avoid unnecessary production costs. Thin and sensitive components, such as the catalytic-coated-membrane of a fuel cell, can be a weak point regarding the manufacturing or assembly process of fuel cells. It is known that the technical cleanliness of fuel cells can be a significant influence in production regarding the quality of components and too many or to big particles may damage the material and cause a lack of performance or even lead to a failure in the system. As the level of knowledge regarding the effect of particles to fuel cell components is low, the focus of this work is to determine a necessary cleanliness level in the production of fuel cells in order to reduce the costs caused by excessive cleaning. Therefore, a system was developed to press particles of different sizes and shapes into the different materials as part of a methodical test procedure and examining the resulting damage using static pressure. The tests reveal that round particles with a high hardness have the most impact on the materials as they penetrate punctual compared to angular particles. Furthermore, it was demonstrated that the applied pressure has a significant impact on the damages to the material. The defects on the gas diffusion layers occurred faster while the catalytic coated membrane was only harmed by big particles.

© 2025 The Authors. Published by Elsevier B.V.
This is an open access article under the CC BY-NC-ND license (https://creativecommons.org/licenses/by-nc-nd/4.0)
Peer-review under responsibility of the scientific committee of the 18th CIRP Conference on Intelligent Computation in Manufacturing Engineering (CIRP ICME ‘24)

Keywords: fuel cell, damage, defect, quality, technical cleanliness, contaminations, effects of defects

1. Introduction

In order to reduce the effects on the climate, the European Union has declared to prevent the emission of environmentally harmful greenhouse gases [1]. One of the challenges to achieving this goal is to store and distribute sufficient energy from renewable sources to become independent of fossil fuels, due to their negative impact on climate change. Although the demand in energy of the G7 countries declined over the past years [2], the biggest part of energy consumption are still fossil fuels [3]. One promising technology to replace fossil fuels in many applications are proton exchange membrane fuel cells (PEMFC) due to their potential use in the mobility sector and stationary power generation [4, 5]. In particular, the ability to refill tanks quickly, the low power-to-weight ratio, and scalability make fuel cells attractive for mobile vehicles such as cars, trucks, ships, or trains [6–9]. However, one of the problems with the substitution of fossil fuels by fuel cells is that the costs per kilowatt have to be lowered to achieve an economic viability [10]. To lower the costs of a fuel cell (FC) per kilowatt either the production must get cheaper, or the performance of the components must rise.

2212-8271 © 2025 The Authors. Published by Elsevier B.V.
This is an open access article under the CC BY-NC-ND license (https://creativecommons.org/licenses/by-nc-nd/4.0)
Peer-review under responsibility of the scientific committee of the 18th CIRP Conference on Intelligent Computation in Manufacturing Engineering (CIRP ICME ‘24)
10.1016/j.procir.2026.01.193

The overall costs of a fuel cell are driven by the production expenses. Depending on the number of units produced annually, over 60% of the costs are attributable to the material used to manufacture the components and around one third to production [11]. The catalytic coated membrane (CCM) is by far the most expensive component due to the necessity of platinum as a catalyst [4]. Despite ongoing research activities on platinum-free catalysts, their inferior performance acts as a barrier to the adoption of alternative materials [12, 13].

Another approach to reduce costs in production is to scale up the produced units as the expenses for manufacturing would get significant lower [11]. This means that manufacturing processes need to produce components at a higher rate with the same quality demands as low-rate production.

Technical cleanliness is one of the critical quality criteria in modern production processes [14]. This is because contaminations such as particles that are unintentionally introduced into production may harm the product and therefore must be removed or prevented [15]. The components of the fuel cell are nowadays very thin, for example the thickness of the proton exchange membrane used in this work is only 50 µm. During assembly, if particles become trapped between components and are pressed together, defects like holes, dents, scratches, or cracks occur in the thin material or the coating. These defects may harm the stability, power and lifetime by thermal, chemical and mechanical degradation mechanisms [16].

Particles originate from various sources like personnel, machine emissions or friction [15]. With a higher production rate and larger plants, the occurrence of particles in the factory is likely to increase as more friction occurs and more personnel as well as machines are required. In order to design production in accordance with the required technical cleanliness and to take the right measures, it is necessary to know which particles are critical for the product and which cleaning systems are suitable for removing these contaminants. Therefore, the objective of this work is to establish an approach for determining a threshold value for particle sizes in fuel cell production.

Nomenclature

BPP	bipolar plate
CCM	catalytic coated layer
FC	fuel cell
GDL	gas diffusion layer
PEMFC	proton exchange membrane fuel cell
PTFE	polytetrafluoroethylene

2. Experimental

2.1. Construction of a material press

To examine the effects of particles pressed into the material, a pneumatic stamping system was constructed (see Fig. 1). A pneumatic cylinder was thus positioned between a static structure comprising a static structure consisting of a top plate and a ground plate connected with threated rods. The threated rods are used to adjust the distance of the system and to level it.

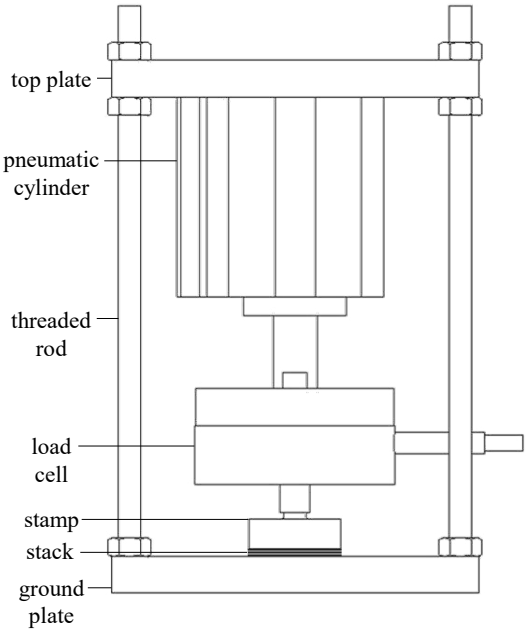

Fig. 1. System to apply a homogeneous pressure to a experimental FC-Stack

The pressure is applied to the material by a stamp which presses towards the ground plate. The stamp was polished to guarantee an even pressure distribution to the material. Between the pneumatic cylinder and the stamp, a load cell manufactured by Burster is placed to measure the applied force to the stamp as the pneumatic pressure is adjusted with an analog manometer at the pressure valve. The load cell is designed for 1 kN and is connected to a computer with Burster DigiVision software.

Typical mechanical pressures in fuel cells vary depending on the system used. Fuel cell stacks are clamped together with a pressure between 2 to 4 MPa to prevent hydrogen leakage and to assure the electrochemical function [17–19]. Furthermore, the structure of the bipolarplate (BPP) results in a inhomogeneous pressure distribution which results in pressure peaks [20].

The available pneumatic pressure for the cylinder was about 1 MPa and therefore had to be extended. Therefore, the diameter of the stamp was calculated in order to be able to press with up to 4 MPa. As the force between the pneumatic cylinder and the stamp (F_p) is the same, the resulting stamp area (A_s) can be calculated multiplying the cylinder pressure (p_c) to stamp pressure (p_s) with the area of the cylinder (A_c).

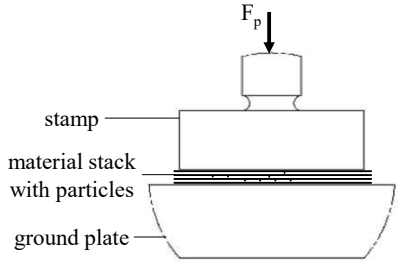

Fig. 2. Principle of the force applied to the material stack.

As the diameter of the pneumatic cylinder (d_c) was chosen to be 32 mm, the diameter of the stamp (d_s) can be calculated by setting multiplying d_c with the ratio of pneumatic pressure (p_p) to the stamp pressure (p_s).

$$F_p = p_c \cdot A_c = p_s \cdot A_s \quad (1)$$

$$A_s = \frac{p_c}{p_s} \cdot A_c = \frac{p_c}{p_s} \cdot \left(\frac{d_c}{2}\right)^2 \cdot \pi \quad (2)$$

With A_s the diameter of the stamp can be calculated:

$$d_s = \sqrt{\frac{A_s * 4}{\pi}} \quad (3)$$

The diameter d_s was chosen to be 15 mm to compensate friction in the system and to reach higher pressures if needed.

The pressure was calculated with the measured force F_p at the load cell and d_s (see Fig. 2). The applied pressures were raised in steps of 0.5 MPa from 2.0 to 4.0 MPa (see Table 1) because of the typical pressure in PEMFC (see 2.1).

Table 1. Stamp pressure to force relation.

stamp pressure p_s (MPa)	2.0	2.5	3.0	3.5	4.0
applied force F_p (N)	354	443	531	620	708

To calibrate the stamp and validate the pressure in the system, pressure measurement film (Fujifilm LW/LLW) was inserted between the ground plate and the stamp. The color of the film changes to a deeper red with increased force. Fig. 3 illustrates an inhomogeneous distribution of the force because of the surface irregularities (a) and bad leveling (b) which were corrected to achieve a homogenous pressure distribution (c). By scanning the films and the indicator scale into a picture, the color intensity could be measured with ImageJ.

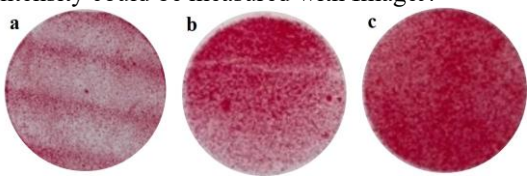

Fig. 3. Pressure distribution between the stamp and the ground plate (a) irregular surface; (b) bad leveling; (c) homogenous pressure.

2.2. Materials

To conduct the experiments materials for a small PEMFC-stack were chosen. Each stack consists of two BPP on top and bottom and one CCM in the middle. A gas diffusion layer (GDL) was placed between the BPP and CCM. The components were cut to have a side length of 15 mm to fit them under the stamp. The BPP material was produced by Fraunhofer UMSICHT from a carbon-polymer-compound. The GDL was a polytetrafluoroethylene (PTFE) coated carbon fabric paper and the CCM was platinum coated Nafion®.

As typical particles in manufacturing often result from the materials used to manufacture the product, the particles used to conduct the experiments were chosen according to the used components.

Table 2. Components used to build a PEMFC-stack.

component	material
BPP	carbon polymer compound (Fraunhofer UMSICHT)
GDL	PTFE coated carbon fabric paper (H23 C6; hot pressed)
CCM	platinum-catalyst coated Nafion® 212 (cathode: 0,6 mg/cm² Pt; anode: 0,3 mg/cm² Pt)

Compound material from the BPP and metallic particles were chosen. For this, the compound material was given into a blender to crush it into small particles. Subsequently, the particles were sieved to separate them into different size fractions for examining the influence of particle diameter. The size fractions where targeted according to ISO 16232 (also VDA Volume 19 part 1) due to the widespread application of this guideline [21, 22]. The size classes were 25-50 µm, 50-100 µm and 100-150 µm. Particles smaller than 25 µm were excluded as they couldn't be prevented during material handling. As PEMFC components are mostly produced in a cleanroom or micro-environment, particles above 150 µm should not be accepted.

Table 3. Particle size classes according to ISO 16232 [22]

particle size class	B	C	D
particle size (µm)	25-50	50-100	100-150

Additionally, as the BPP can also be made of metal, metallic particles were produced to compare the influence of the particle hardness. Since blending metal was not feasible, the particles were collected using a magnet in a sandblasting machine and subsequently sieved. The particles collected contained different materials and were analyzed with EDX, were mostly Fe, Al and Cu could be found in addition to various alloy-materials. Based on this analysis and the materials subjected to sandblasting in the machine, it can be inferred that the particles originate from Fe-, Al- and Cu-alloys (e. g. 1.4404, AlSi10Mg or CuCr1Zn).

To compare the influence of the morphology of the particles, round particles where also used. Therefore, 1.4404-powder from additive manufacturing was sieved in the same fractions as the other particles. Powder used in additive manufacturing is usually atomized and therefore round.

Table 4. Particle morphology and material

type	morphology	material
compound	angular	carbon polymer compound
metal	angular	mixed Fe-, Al- and Cu-alloys
metal	round	1.4404

The particles were then suspended in isopropanol to apply them with a pipette evenly between the layers. As the CCM is not resistant to isopropanol, a droplet of the suspension was given to the GDL and after drying the stack could be assembled. By applying the particles with droplets an even and homogeneous distribution on the surface could be achieved. Furthermore, as each droplet contains a high number of particles, each stack could be used to analyze a wide range of

the particle's effects. The material was then placed between the stamp and the ground plate, the air pressure was then slowly raised with the pneumatic valve until the needed stamp pressure was reached. For every size class, every particle type and every pressure applied, the effect of the particles on each side of the CCM and two GDL was analyzed.

3. Results and discussion

An optical microscope was used to analyze the material regarding the defects. Subsequently, the stacks were positioned under the lens, and the layers were meticulously removed to expose the particles once more. The particles were then removed individually with a small brush to prevent the surface from being scratched by this procedure. The defects are visually categorized based to the categories of DIN EN ISO 8785, which gives the categories of surface imperfections [23]. For the conducted experiments four cases where expected: marks, indentations, dents, and cracks (see Fig. 4).

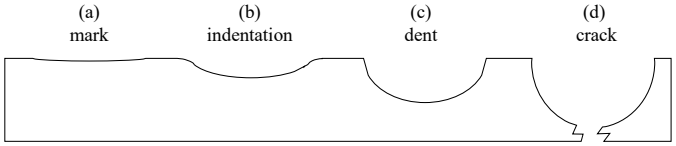

Fig. 4. Defect dimensions

When nothing or only light marks can be found (Fig. 4-a), without noticeable depth, no defect was classified. Indentations on the other hand (Fig. 4-b) are still noticed but have a low impact deep and show a smooth transition from non-defected areas to defected areas. Dents can be identified when the particles deformed the surface in a significant way and hard edges can be seen under the microscope (Fig. 4-c). Cracks or comparable defects through the material show open spots through the material (Fig. 4-d). As the criticality increases from a to d, marks and indentations were categorized as "no defects", dents where categorized as "slight defects" and cracks are "severe defects".

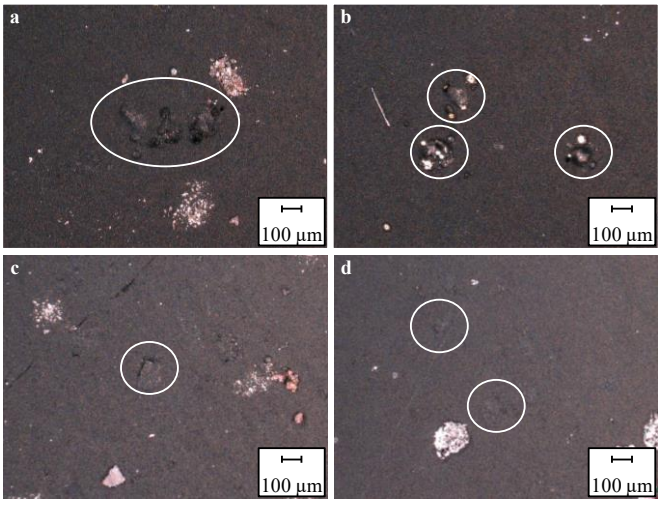

Fig. 5. Defects on GDL resulted by class D particles (a) metallic-angular at 4 MPa; (b) metallic-round at 4 MPa; (c) metallic-angular at 2 MPa; (d) compound class B at 2,5 MPa.

Fig. 5 shows extracts of the experiments conducted with the GDL. Severe damages can be found for all metallic-round particles, independent of the applied pressure (Fig. 5-b). Angular metal particles on the other hand showed pressure related defects (Fig. 5-a). Below 3.0 MPa only slight defects occurred (Fig. 5-c) and above they were also severe (Fig. 5-b). Compound particles on the other hand show no damages at all below 3.0 MPa (Fig. 5-d), slight defects until 3.5 MPa and above also severe damages.

Table 5 shows the defect-categorization on the GDL at every test conducted.

Table 5. Defects on the GDL

pressure (MPa)	particle size class	defects caused by		
		metallic round particles	metallic angular particles	compound angular particles
2.0	B	2	1	0
	C	2	1	0
	D	2	1	0
2.5	B	2	1	0
	C	2	1	0
	D	2	1	0
3.0	B	2	2	1
	C	2	2	1
	D	2	2	1
3.5	B	2	2	1
	C	2	2	1
	D	2	2	1
4.0	B	2	2	2
	C	2	2	2
	D	2	2	2

"0" = no defect; "1" = slight defect; "2" = severe defect

The different results between the particle morphology and material can mainly be explained by two aspects: the hardness and the force impact on the surface. The metallic particles are relatively hard compared to the compound particles and therefore exhibit less deformation when force is applied. The contact area increases, and the compound adapts to the surface by flattening. However, metal does not deform as much and therefore applies a more punctual force to the GDL. The same principle happens when using round particles as the contact surface is lower and so the force distribution to the surface is lower. If the elastic deformation limit of the PTFE coating is exceeded, the force will result in a dent. By applying more force (or the same pressure more punctual), the plastic deformation capacity will at some point end and result in a crack. PTFE is rather brittle, and the region of plastic deformation is only short, which is why it breaks directly.

The CCM, despite their low thickness, was damaged way less compared to the GDL. No effects could be seen unless when 4.0 MPa were applied to the material with round particles of 100-150 µm. Fig. 6-a/b shows that even bigger compound-particles do not result in a damage. Although the particle seen in Fig. 6-a is longer than 150 µm, it is less than 150 µm in width

and flattens to the surface when pressure is applied. Fig. 6-b shows the same spot without any mark, after removing the particle with a brush. Metallic-round particles cause light marks when proceeding the same way (Fig. 6-c/d).

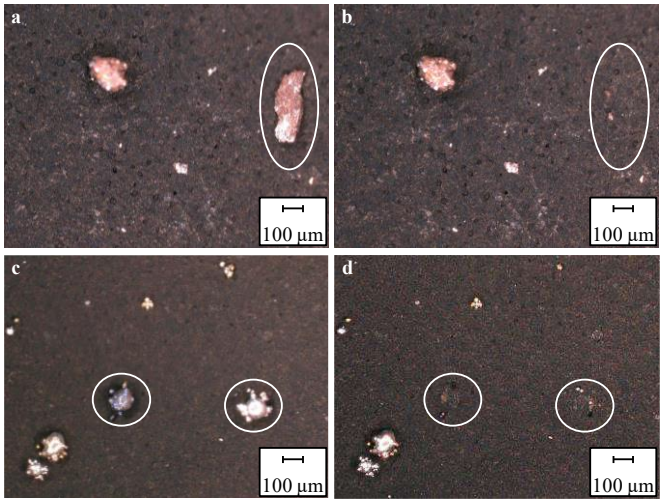

Fig. 6. Defects on CCM resulted by class D metallic particles at 4 MPa before (a/c) and after (b/d) removing angular (a/b) and round (c/d) particles.

Lower pressures, smaller particles and other particle material or morphology had no visual influence on the surface. One explanation could be the elastic and plastic deformation property of the material, thus no severe defect was observable. Furthermore, the weakest material in the stack is the first to show damage, which in this case is the GDL.

Table 6. Defects on the CCM

pressure (MPa)	particle size class	defects caused by		
		metallic round particles	metallic angular particles	compound angular particles
2.0	B	0	0	0
	C	0	0	0
	D	0	0	0
2.5	B	0	0	0
	C	0	0	0
	D	0	0	0
3.0	B	0	0	0
	C	0	0	0
	D	0	0	0
3.5	B	0	0	0
	C	0	0	0
	D	0	0	0
4.0	B	0	0	0
	C	0	0	0
	D	1	0	0

"0" = no defect; "1" = slight defect; "2" = severe defect

Table 6 shows the defect-categorization on the GDL at every test conducted. Regarding the BPP and its PVD coating no effects of the test could be observed due to the relatively high hardness compared to the GDL and CCM. Therefore, no further tests were conducted.

However, none of the trials showed pinholes or cracks through the GDL or CCM, which means that no serious restrictions to the functionality are expected.

4. Conclusion

The experiments conducted in this work showed that contaminations may harm the surface of fuel cell components. When pressure was applied to the material with particles trapped between the layers, defects could be found depending on the particles size, morphology, and material. Also, the mechanical pressure has a significant influence. However, no serious damages like pinholes or cracks through the whole material were seen.

To determine a cleanliness level for the products the critical particles for the weakest material has to be taken as the CCM touches the GDL directly. Therefore, both components have to be clean before stacking the fuel cell. Regarding the conducted test, the necessary cleanliness level for the examined materials is depending on the pressure applied to the stack. If the cleanliness cannot be ensured, a cleaning process must be integrated in the production. Additionally, a concept to prevent contaminations by the surrounding (e.g., personal or logistic) can be implemented in the production. If high cleanliness levels are necessary, a structural measure like clean rooms have to be considered. Another possibility could be to lower the cleanliness limits in the production due to the low effects seen in the experiments.

As the experiments showed no critical defect, like pinholes or cracks, bigger particles than 200 µm were applied for further investigation. Severe cracks in the coating can be seen, but no holes through the whole material. Nevertheless, bigger particles are expected to cause critical damages when applied with high pressures and therefore must be prevented in the production.

Although damages could be observed on the material, the influence on the performance of a fuel cell was not examined, neither in short term nor in long term. It might be possible that the functionality is not affected significantly by small dents or cracks in the surface. Furthermore, only static experiments were conducted, and no dynamic force was applied. As fuel cells might vibrate in operation, particles may harm the surface more. In addition to the force or pressure behavior, internal factors like temperature or humidity are also expected to have a significant impact on the deformation behavior. Therefore, further experiments need to be conducted to get a better understanding on the effects of contaminations in the fuel cell. It is also known that some materials (e.g., copper) have a negative electrochemical influence on the materials of a fuel cell and therefore must be considered separately.

Acknowledgements

This work was funded by the Federal Ministry for Digital and Transport of Germany (BMDV), coordinated by the National Organisation Hydrogen and Fuel Cell Technology (NOW) and Project Management Jülich (PtJ). We also thank

our colleges from Fraunhofer UMSICHT and Fraunhofer IWU for the material samples used in this work.

References

[1] United Nations, 2015. Paris Agreement to the United Nations Framework Convention on Climate Change: UNFCCC.
[2] Xing, H., Husain, S., Simionescu, M., Ghosh, S. et al., 2024. Role of green innovation technologies and urbanization growth for energy demand: Contextual evidence from G7 countries 129, p. 220.
[3] Suzuki, M., Jewell, J., Cherp, A., 2023. Have climate policies accelerated energy transitions? Historical evolution of electricity mix in the G7 and the EU compared to net-zero targets 106, p. 103281.
[4] Kahraman, H., Akın, Y., 2024. Recent studies on proton exchange membrane fuel cell components, review of the literature 304, p. 118244.
[5] Abdelkareem, M.A., Elsaid, K., Wilberforce, T., Kamil, M. et al., 2021. Environmental aspects of fuel cells: A review. Sci Total Environ 752, p. 141803.
[6] Fu, Z., Lu, L., Zhang, C., Xu, Q. et al., 2023. Fuel cell and hydrogen in maritime application: A review on aspects of technology, cost and regulations 57, p. 103181.
[7] Luo, Y., Wu, Y., Li, B., Mo, T. et al., 2021. Development and application of fuel cells in the automobile industry 42, p. 103124.
[8] Ding, D., Wu, X.-Y., 2024. Hydrogen fuel cell electric trains: Technologies, current status, and future 17, p. 100255.
[9] Anselma, P.G., Belingardi, G., 2022. Fuel cell electrified propulsion systems for long-haul heavy-duty trucks: present and future cost-oriented sizing 321, p. 119354.
[10] Burke, A.F., Zhao, J., Miller, M.R., Sinha, A. et al., 2023. Projections of the costs of medium- and heavy-duty battery-electric and fuel cell vehicles (2020-2040) and related economic issues 77, p. 101343.
[11] Kampker, A., Heimes, H., Kehrer, M., Hagedorn, S. et al., 2023. Fuel cell system production cost modeling and analysis 9, p. 248.
[12] Lin, P.Z., Sun, J., He, C.X., Wu, M.C. et al., 2024. Modeling proton exchange membrane fuel cells with platinum-group-metal-free catalysts 360, p. 122765.
[13] Xu, X., Kang, N., Zulevi, B., Serov, A. et al., 2023. Highly durable platinum group metal-free catalyst fiber cathode MEAs for proton exchange membrane fuel cells 586, p. 233679.
[14] Tammer, C., Schießl, T., Burgdorf, P., 2023. Brennstoffzelle - wie sauber muss es sein? 63, p. 60.
[15] Oravec, M., Divoková, A., Lipovský, P., Karásek, M. et al., 2019. Technical Cleanliness - a Requirement of Precision Manufacturing 23, p. 46.
[16] Kundu, S., Fowler, M.W., Simon, L.C., Grot, S., 2006. Morphological features (defects) in fuel cell membrane electrode assemblies 157, p. 650.
[17] Elena Borgardt. Mechanische Eigenschaften von katalysatorbeschichteten Membranen für die Polymer-Elektrolyt-Membran Elektrolyse. Forschungszentrum Jülich GmbH, Jülich.
[18] Zhou, Y., Lin, G., Shih, A.J., Hu, S.J., 2009. Multiphysics Modeling of Assembly Pressure Effects on Proton Exchange Membrane Fuel Cell Performance 6, p. 2334.
[19] Li, S., Sundén, B., 2018. Effects of gas diffusion layer deformation on the transport phenomena and performance of PEM fuel cells with interdigitated flow fields 43, p. 16279.
[20] Wang, X., Song, Y., Zhang, B., 2008. Experimental study on clamping pressure distribution in PEM fuel cells 179, p. 305.
[21] VDA Verband der Automobilindustrie e.V. Prüfung der Technischen Sauberkeit: Partikelverunreinigungen funktionsrelevanter Automobilteile, 2nd edn., Berlin. VDA/QMC, 2015(VDA Band 19 Teil 1).
[22] ISO International Organization for Standardization. Road vehicles: Cleanliness of components and systems, Berlin. Beuth Verlag 13.040.50, 43.180(ISO 16232:2018(E)).
[23] DIN Deutsches Institut für Normung e.V. Oberflächenunvollkommenheiten: Begriffe, Definitionen und Kenngrößen, 1999th edn. 01.040.17; 17.040.20, 1999(DIN EN ISO 8785)..